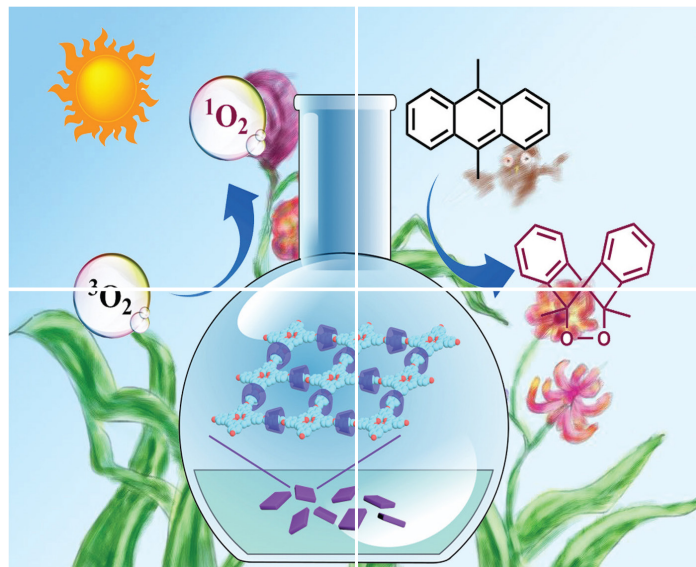


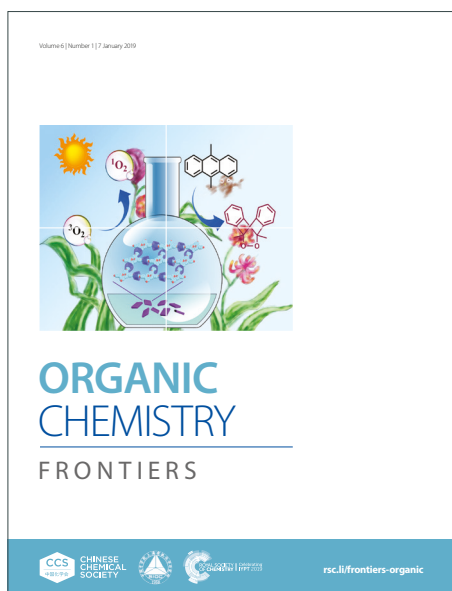
# ORGANIC CHEMISTRY

## FRONTIERS

Accepted Manuscript



This article can be cited before page numbers have been issued, to do this please use: S. Mkrtchyan, G. Addová, J. Filo, K. Ayub, M. G. Garcia, S. S. Khutsishvili, Y. Karpun, E. Kupcová, V. B. Purohit, S. Sarfaraz, M. Shkooor, B. Benicka, O. Shalimov, V. Yepishev, J. Zapletal and V. Iaroshenko, *Org. Chem. Front.*, 2025, DOI: 10.1039/D5QO01041A.



This is an Accepted Manuscript, which has been through the Royal Society of Chemistry peer review process and has been accepted for publication.

Accepted Manuscripts are published online shortly after acceptance, before technical editing, formatting and proof reading. Using this free service, authors can make their results available to the community, in citable form, before we publish the edited article. We will replace this Accepted Manuscript with the edited and formatted Advance Article as soon as it is available.

You can find more information about Accepted Manuscripts in the [Information for Authors](#).

Please note that technical editing may introduce minor changes to the text and/or graphics, which may alter content. The journal's standard [Terms & Conditions](#) and the [Ethical guidelines](#) still apply. In no event shall the Royal Society of Chemistry be held responsible for any errors or omissions in this Accepted Manuscript or any consequences arising from the use of any information it contains.

# Mechanochemical Production of Biphenyls from Nitrogen-Containing Organic Compounds: Amides, Anilines, and Sulfonamides

Satenik Mkrtchyan<sup>\*,a,b</sup>, Oleksandr Shalimov,<sup>c</sup> Michael G. Garcia,<sup>d</sup> Sehrish Sarfaraz,<sup>e</sup> Khurshid Ayub,<sup>e</sup> Spartak Khutsishvili,<sup>f</sup> Gabriela Addová,<sup>g</sup> Juraj Filo,<sup>g</sup> Mohanad Shkoor,<sup>h</sup> Vishal B. Purohit,<sup>i</sup> Yevhen Karpun,<sup>j,k</sup> Vitaliy Yepishev,<sup>j</sup> Jiří Zapletal,<sup>a</sup> Elena Kupcová,<sup>a</sup> Barbora Benická,<sup>a</sup> Viktor O. Iaroshenko<sup>\*,a,l,m</sup>

<sup>a</sup>Department of Chemistry, Faculty of Natural Sciences, Matej Bel University, Tajovského 40, 97401, Banská Bystrica, Slovakia.

<sup>b</sup>Georgian American University, School of Medicine, 10 Merab Aleksidze Str., 0160 Tbilisi, Georgia.

<sup>c</sup>Department of Heteroatom Chemistry, Institute of Organic Chemistry, National Academy of Sciences of Ukraine, 5 Murmans'ka, 02660, Kyiv Ukraine.

<sup>d</sup>Department of Biology/Chemistry, Center for Cellular Nanoanalytics (CellNanOs), Universität Osnabrück, Barbarastr. 7, D-49076, Osnabrück, Germany.

<sup>e</sup>Department of Chemistry, COMSATS University, Abbottabad Campus, Abbottabad, KPK, 22060, Pakistan.

<sup>f</sup>R. Agladze Institute of Inorganic Chemistry and Electrochemistry, Ivane Javakhishvili Tbilisi State University, 11 Mindeli St., 0186 Tbilisi, Georgia.

<sup>g</sup>Department of Organic Chemistry, Faculty of Natural Sciences, Comenius University, SK-84215, Bratislava, Slovakia.

<sup>h</sup>Department of Chemistry and Earth Sciences, Qatar University, P.O. Box 2713, Doha, Qatar.

<sup>i</sup>Department of Chemical Sciences, P. D. Patel Institute of Applied Sciences, Charotar University of Science and Technology (CHARUSAT), Changa 388 421, Gujarat, India.

<sup>j</sup>Life Chemicals Ukraine, Winston Churchill St. 5, 02000, Kyiv, Ukraine.

<sup>k</sup>Professional medical and pharmaceutical college (IAPM), Frometivska, 2, Kyiv, 03039, Ukraine.

<sup>l</sup>Functional Materials Group, Gulf University for Science and Technology, Mubarak Al-Abdullah 32093, Kuwait, Kuwait.

<sup>m</sup>Institute of Applied Synthetic Chemistry, TU Wien, Getreidemarkt 9/163-OC, Vienna, 1060 Austria.

\*Corresponding author, Email: [iva108@gmail.com](mailto:iva108@gmail.com), [viktor.iaroshenko@umb.sk](mailto:viktor.iaroshenko@umb.sk), [iaroshenko.V@gust.edu.kw](mailto:iaroshenko.V@gust.edu.kw), [viktor.iaroshenko@tuwien.ac.at](mailto:viktor.iaroshenko@tuwien.ac.at)

**KEYWORDS.** Pyrylium salts, Functionalization, C–N bond activation, Deamination, Boronic acids, Coupling, Mechanochemistry

**ABSTRACT:** The presence of C(sp<sup>2</sup>)–NH<sub>2</sub> in pharmaceutical building blocks provokes a pressing demand for the discovery and development of deaminative functionalization of the C(sp<sup>2</sup>)–NH<sub>2</sub> moiety to enable new routes for late-stage functionalization of complex molecules. In this work, we disclose a mechanochemical deaminative arylation of C(sp<sup>2</sup>)–NH<sub>2</sub> by *in situ* conversion of C(sp<sup>2</sup>)–NH<sub>2</sub> to reactive pyridinium salts *via* selective condensation of C(sp<sup>2</sup>)–NH<sub>2</sub> with pyrylium tetrafluoroborate. Deaminative coupling of anilines, amides, and sulfonamide represents a key development for the selective functionalization process, enabling production of precursor biphenyl compounds with the potential to develop biologically active molecules.

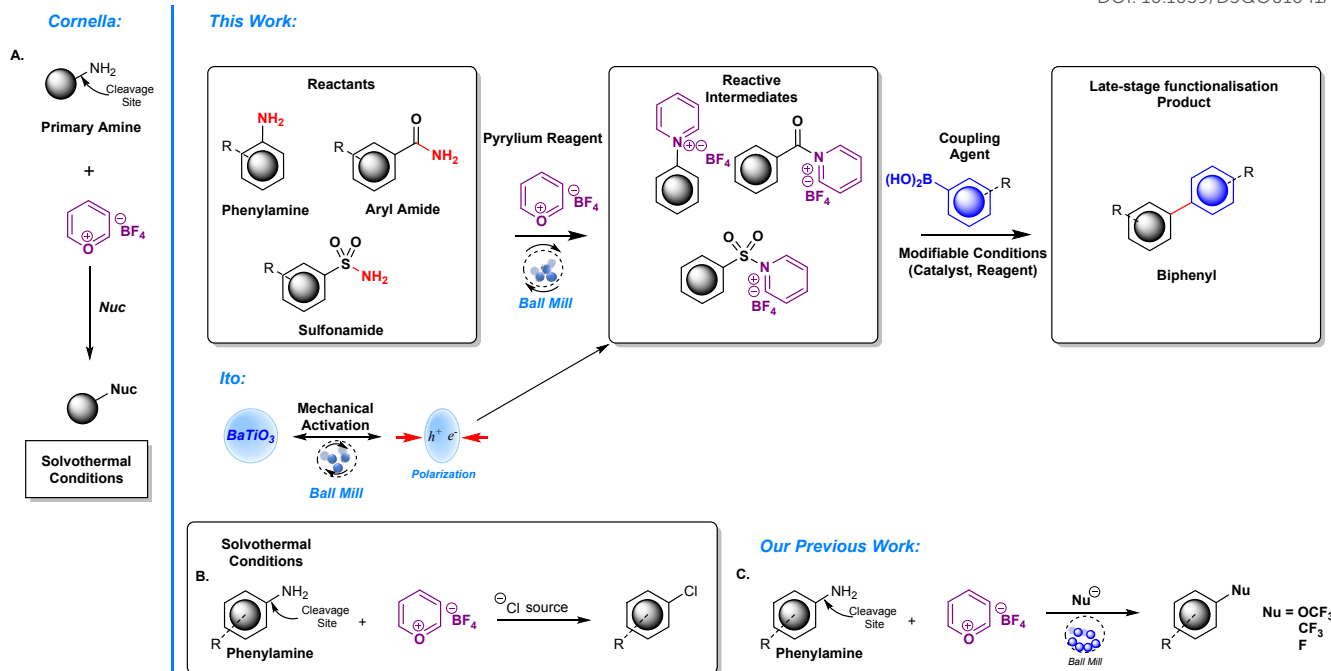
The selective interconversions of functional groups in molecular frameworks are one of the common practices in contemporary synthetic organic chemistry as they provide reliable tools for desired late-stage as well as selective functionalization of organic molecules. These processes also enable the unwavering routes for the construction of complex molecules by connection of abundant building blocks. In this context, the activation of chemically inert bonds has profoundly been the focus of synthetic organic chemists.<sup>1</sup> To this end, several functional groups like carboxylic acids<sup>2, 3</sup>, aryl halides<sup>4</sup>, alcohols<sup>5</sup>, nitriles<sup>6</sup> and organoboron<sup>7, 8</sup> compounds have been routinely utilized as points of connections to streamline the formation of complex molecules. As a result, those functionalities are abundant in medicinal chemistry libraries for drug synthesis.<sup>9-11</sup> Considerable efforts have been made to include other nontraditional functionalities in the library of diversifiable functional groups.<sup>12-17</sup> Primary aromatic amines are prevalent functional group in organic compounds. They are abundant moieties in the scaffold of many natural products, pharmaceuticals, biomolecules, building blocks and other synthetic molecules utilized in various applications.<sup>18</sup> Considering the importance of these molecules, thus, primary aromatic amines have attracted considerable interest as points of functionalization and synthetic disconnections.

However, the interconversion of C(sp<sup>2</sup>)-NH<sub>2</sub> bond into other functionalities remains a persistent challenge due to their low heterolytic nucleofugality, high C-N bond dissociation energy (BDE of C<sub>6</sub>H<sub>5</sub>-NH<sub>2</sub>: 102.6 ± 1.0 kcal/mol)<sup>19</sup>, and basicity.<sup>20-23</sup> In addition, the high affinity of nitrogen lone pair to metals inhibits metals catalyzed activation of C(sp<sup>2</sup>)-NH<sub>2</sub> bond. To overcome these challenges, C(sp<sup>2</sup>)-NH<sub>2</sub> bond activation strategies have relied on interconversion of the amino group into leaving groups via strategies such as diazotization<sup>24, 25</sup> and polyalkylation.<sup>26-30</sup> This implies that the introversion of primary amine functionality requires at least two distinct interconversions. Although there are useful protocols for deaminative functionalization, these protocols involve serious inherent drawbacks such as the thermal instability of the aryl diazonium salts, incompatibility of wide range of functional groups with the highly oxidizing and acidic reaction conditions, and pre-functionalization requirements.

Katritzky group in a groundbreaking work in C(sp<sup>3</sup>)-NH<sub>2</sub> activation demonstrated that primary amines could be converted to pyridinium salts by reaction with pyrylium cations rendering amines as electrophiles for further nucleophilic functionalization reactions.<sup>31-33</sup> This strategy has become an important component in the toolbox of C-N activation since pyridinium salts are air and moisture insensitive, pyrylium salts are chemoselective for primary amines and the tolerance of a wide spectrum of functional groups with the reaction conditions.<sup>34-39</sup>

Organoboron compounds are among the most versatile reagents in organic synthesis. Consequently, organoborons were among the nucleophiles that were employed successfully in Suzuki-Miyaura transition metal catalyzed couplings with pyridinium salts to create C-C bonds. However, these couplings were restricted to *N*-alkylpyridinium salts<sup>40, 41</sup> and benzylic pyridinium salts<sup>42, 43</sup> due to the relatively lower BDE of C(sp<sup>3</sup>)-NH<sub>2</sub> compared to C(sp<sup>2</sup>)-NH<sub>2</sub> bond, (CH<sub>3</sub>-NH<sub>2</sub>: 85.1 ± 0.5 kcal/mol).<sup>19</sup> However, Activation of the C(sp<sup>2</sup>)-NH<sub>2</sub> bond is more challenging which explains why C(sp<sup>2</sup>)-NH<sub>2</sub> deaminative coupling with organoboron reagents has not been studied.

Recently, a new advancement in the field of C(sp<sup>2</sup>)-NH<sub>2</sub> activation was reported by Cornella in which deaminative functionalization via an S<sub>N</sub>Ar mechanism was realized in a single step by *in situ* formation of pyridinium ion (**Scheme 1A** and **1B**).<sup>44-47</sup> Inspired by this work, our group has reported the mechanochemically induced selective interconversion of primary aromatic amino group into OCF<sub>3</sub>, CF<sub>3</sub> and F functionalities by *in situ* condensation of C(sp<sup>2</sup>)-NH<sub>2</sub> with pyrylium reagent (Pyr-BF<sub>4</sub>) to create the pyridinium salts followed by S<sub>N</sub>Ar reaction with the respective fluoro surrogates (**Scheme 1C**).<sup>48-50</sup>



**Scheme 1.** Illustration of the basis employed for developing targeted mechanistic deaminative coupling along our previous work and current results.

Following our research of harnessing mechanochemically triggered transformations of traditionally, chemically inert bonds<sup>12, 48, 51, 52</sup>, we would like to report here our result in C–C bond formation through coupling of C(sp<sup>2</sup>)–NH<sub>2</sub> sites in anilines, amides, and sulfonamides. Our investigation was centered on the deaminative functionalization using pyrylium tetrafluoroborate, incorporating a mechanochemical protocol pioneered independently by Hernández, Bolm and Hajime Ito. In this manner, amine functional groups are activated via complexation with the pyrylium tetrafluoroborate to provide the key reactive pyridinium salt intermediates (**Scheme 1**).<sup>32, 47, 48, 51</sup> The process is enabled by the piezoelectric BaTiO<sub>3</sub> material through a ball milling process which provides the necessary energy to bypass activation barriers and propel the reaction forward<sup>53–55</sup> and further investigation by Ito revealed that a synergy BaTiO<sub>3</sub> and DABCO under ball-milling conditions offered a mechanoredox system for C–N cross-coupling reactions.<sup>53</sup> Methodologies then move on to a vital advancement step: the transition-metal-free coupling with the corresponding pyridinium salt intermediate of anilines<sup>24, 48</sup> while in case of amides and sulfonamides the presence of transition metal is mandatory. By design, the elimination of pre-functionalization of substrates under transition metal-free/ catalyzed solvent-less mechanochemical conditions in this crucial transformation underscores the environmentally benign and sustainable nature of our methodology in line with green chemistry principles.<sup>56, 57</sup> This novel methodology provides a more efficient approach to synthesize complex molecules but also had a multiplicatively beneficial effect on efficiency in the reaction yield. This method is, therefore, of much importance in organic chemistry since it utilizes cheap and readily available starting materials and rules out environmentally hazardous halogenated reagents/starting materials widely employed for cross-coupling reactions.<sup>58, 59</sup> It offers a powerful method for producing biphenyl structures through a sustainable and environmentally benign pathway, marking a notable advancement in the field.

## Results and Discussion

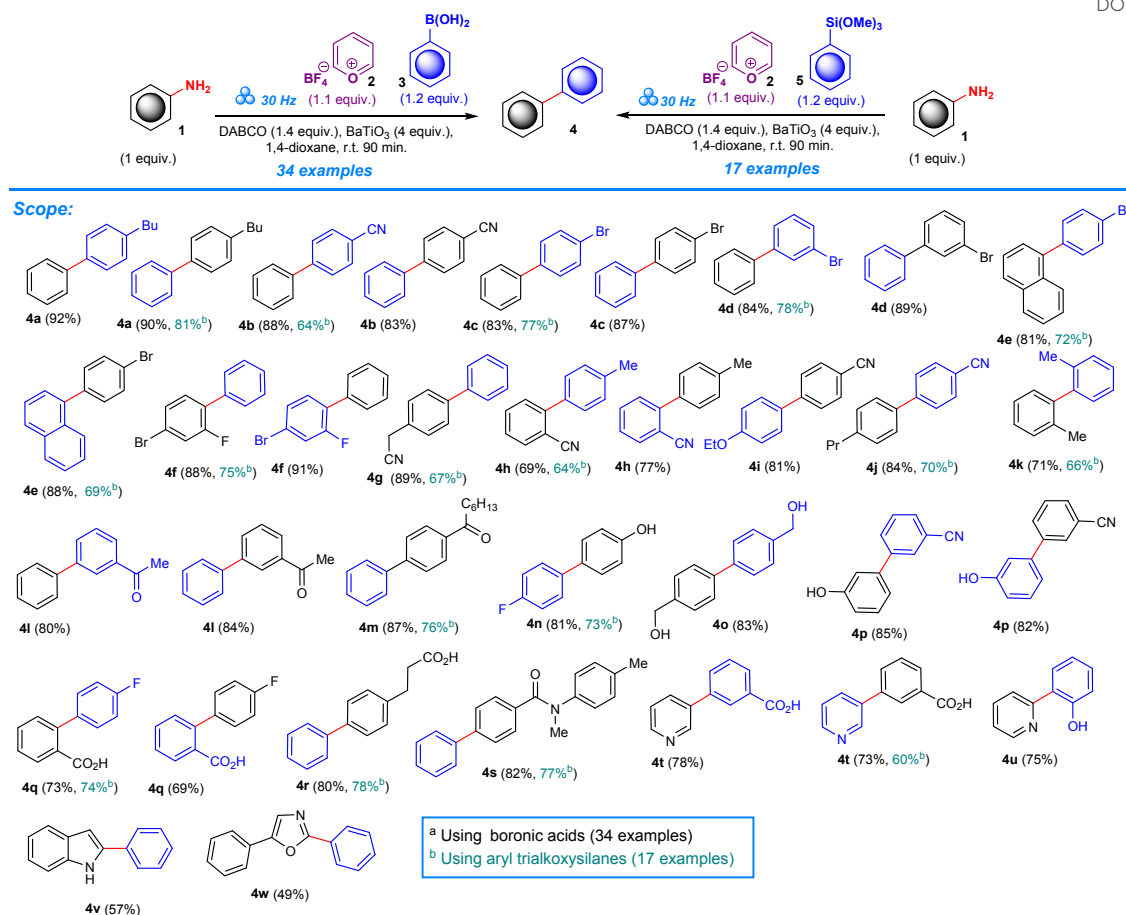
Herein, on the platform of mechanochemical transformations in organic synthesis, we report a new C–C bond formation via coupling of C(sp<sup>2</sup>)–NH<sub>2</sub> with boronic acids and aryltrialkoxysilanes. (**Scheme 2**). In tandem, we developed a protocol for the deaminative functionalization of amides and sulfonamides *via* extrusion of the carbonyl /sulfonyl moiety induced by organometallic catalysis, leading to the production of biphenyls. (**Scheme 3 and 4**).

In the framework of the study, a set of solid-phase reactions was carried out in a systematized way in order to discern the influence of the application of different kinds of additives on the yield. Samples of anilines **1**, pyrylium tetrafluoroborate **2**, and boronic acids **3** (or trialkoxysilanes, **5**) in the ratio of 1 equivalent, 1.1 equivalent, 1.2 equivalent, respectively, were milled at 30 Hz for 90 minutes<sup>60</sup> with the addition of 0.20 mL of 1,4-dioxane as a liquid-assisted grinding (LAG) additive.<sup>61</sup>

The variation was introduced by the addition of 4 equivalents of BaTiO<sub>3</sub>, alone or in the presence of 1.4 equivalents of various nucleophilic enhancers: Na<sub>2</sub>CO<sub>3</sub>, K<sub>2</sub>CO<sub>3</sub>, Cs<sub>2</sub>CO<sub>3</sub>, NEt<sub>3</sub> (triethylamine), (iPr)<sub>2</sub>NEt (Diisopropylethylamine), DABCO. See **Tables S1** and **S2**. The yields by the different types of additives used with reactants are those of reactions that are conducted in a series of experiments that boronic acids could result in, as **Table S1** below states. Without additives, 0% yield was obtained (**Table S1, entry 1**). With BaTiO<sub>3</sub>, results started to appear with a 17% yield (**Table S1, entry 2**). After that, with BaTiO<sub>3</sub> separately, no yields had been observed after adding Na<sub>2</sub>CO<sub>3</sub>, K<sub>2</sub>CO<sub>3</sub>, and Cs<sub>2</sub>CO<sub>3</sub> (**Table S1, entries 3-5**). With BaTiO<sub>3</sub> in combination with NEt<sub>3</sub> and (iPr)<sub>2</sub>NEt, the yield was 48% and 43%, respectively (**Table S1, entries 6-7**). The use of DABCO under the influence of BaTiO<sub>3</sub> afforded the best yield of 92% (**Table S1, entry 8**). For the set of experiments with trialkoxysilane from **Table S2**, a similar trend in yields was observed, but with slight deviations. The presence of BaTiO<sub>3</sub> by itself affected neither on the yield of the desired product—the yield was 0% for all the modifications (**Table S2, entries 1-2**). The individual introduction of BaTiO<sub>3</sub> with Na<sub>2</sub>CO<sub>3</sub>, K<sub>2</sub>CO<sub>3</sub>, Cs<sub>2</sub>CO<sub>3</sub>, or NEt<sub>3</sub> maintained a yield of 0%, signifying product absence within these parameters (**Table S2, entries 3-6**). Introducing (iPr)<sub>2</sub>NEt with BaTiO<sub>3</sub> proved otherwise, and the combination resulted in a 33% yield (**Table S2, entry 7**). The maximum yield of 81% was achieved when the combination of DABCO and BaTiO<sub>3</sub> was used conjunctly, **Table S2** – entry 8, indicating that it was far more effective for the preparation of the target compound compared to all other combinations tried in this series. In the preliminary stage of work, a control reaction was carried out without applying any additive, **Table S1** and **S2** – entry 2. This offered a direct measurement of the impact the addition of additives would have on the efficiency of the reaction. After that, the addition of BaTiO<sub>3</sub> in combination with additives that act as furnishers of nucleophilic enhancement, offered a mixed performance for individual entries. For all those experiments which employed carbonate reagents containing reactions incorporating Na<sub>2</sub>CO<sub>3</sub>, K<sub>2</sub>CO<sub>3</sub>, and Cs<sub>2</sub>CO<sub>3</sub> (**Table S1** and **S2, entries 3-5**), our experimental setups registered no product in the reaction yields. Hindered organic bases, for example, NEt<sub>3</sub>, (iPr)<sub>2</sub>NEt, and DABCO, were tested for their capacity to increase product efficiency. DABCO emerged as the most efficient variable to maximize yield in both series of **Table S1** and **S2**, with a relatively diminished efficiency in series of **Table S2** by trialkoxysilanes. After the best reaction conditions had been established, we planned another control experiment to verify the efficiency of our procedure in the absence of either 1,4-dioxane or the LAG additive. In both series, **Table S1** and **S2**, it was observed that the yield had dramatically dropped. For boronic acids, this decreased to 35% (**Table S1, entry 9**), whereas for the trialkoxysilanes, the yield decreased to 48% (**Table S2, entry 9**). Within this array of additives, there is an increasing order of mild to highly potent bases and nucleophilic catalysts. First, carbonates like Na<sub>2</sub>CO<sub>3</sub>, K<sub>2</sub>CO<sub>3</sub>, and Cs<sub>2</sub>CO<sub>3</sub> are typical weak bases.<sup>62</sup> As the sequence progresses, more nucleophilic catalysts and more potent bases come into play, followed by NEt<sub>3</sub>, NEt<sub>2</sub>Ph, and (iPr)<sub>2</sub>NEt. It is here, of course, that steric hindrance is significantly enhanced in this sequence, highly pronounced in species such as (iPr)<sub>2</sub>NEt. This is articulated clearly by including complex, highly nucleophilic compounds, like DABCO, already known for playing a key role in the elevation of nucleophilicity in the series which impacts on efficiency and yield of the reactions. In previous works, DABCO is used in the mechanochemical C–N bond formation reactions by the Ito group to obtain high yields with a nickel(II) catalyst and piezoelectric material under ball-milling conditions.<sup>53</sup> Moreover, in our previous studies has shown a remarkable potential to be used as a base in a variety of mechanochemically induced cross-coupling reactions. In this regard, this developed approach inspired us to devise an effective manner of securing success in our reaction.

Another series of control experiments focused our attention on highlighting the importance of a solid-phase, mechanochemical environment for reaction completion and the formation of products. The reactions were carried out with each of them comprising one equivalent of reactant **1**, 1.1 equivalents of reactant **2**, 1.3 equivalents of reactant **3** or **5**, 1.4 equivalents of DABCO additions, and then 4 equivalents of BaTiO<sub>3</sub>. Each of the experimental entries used different solvents and temperature conditions to establish the effect of this reaction and the formation efficiency of this product: the first entry utilized the solvent methanol, and the reaction mixture went under reflux for 24 h (**Table S1** and **S2, entry 10**). Similarly, using the solvent acetonitrile, 1,4-dioxane and THF, each of the following entries were reacted under reflux for a 24-hour period (**Table S1** and **S2, entries 11-13**). Although a high degree of solvent variation occurs here, the yields in all these entries were 0%, denoting no visible completion of reaction or product formation under the conditions applied. Other experiments examined the temperature parameters for the dimethylformamide (DMF) solvent. The reaction mixtures were subjected to 100 °C and 130 °C, respectively (**Table S1** and **S2, entries 14-15**). After being kept in such conditions for 24 h, along with the optimal molar ratios, such changes in the reaction conditions resulted in a 0% yield. The uniform yield across all the experimental setups was 0%, which indicated the reaction did not proceed as expectedly; nothing seemed to generate products across different solvent systems, despite the alterations to the experimental conditions—very much in contrast to what could be obtained with mechanochemical conditions. The success of our approach relies critically on the presence of BaTiO<sub>3</sub>, which is known to exhibit piezoelectric properties. BaTiO<sub>3</sub> requires activation through mechanical stimuli; this process induces structural deformation which leads to the formation of temporary polarized particles.<sup>55</sup> The effectiveness of the mechanical stress applied to BaTiO<sub>3</sub> relies on the size, frequency, and number of ball milling equipment, a solvent-based systems is unable to deliver the necessary mechanical energy to change the BaTiO<sub>3</sub> structure. Consequently, mechanochemical approaches become crucial to providing successfully coupled reactions in this structure case.



**Scheme 2.** Scope of biphenyls.

A broad reaction scope was established (**Scheme 2**), in which correlation of high yields depend on the positions of substituents on the aniline-derivative reactants and the coupling reagents used—boronic acids and trialkoxysilanes. A variety of products from the reaction of para-substituted reagents and boronic acids were viewed to correlate with the higher efficiency. With a trend characterized by a high yield, product yields for **4a–4c**, **4e**, **4g**, **4i**, **4j**, **4m–4o**, **4r**, and **4s** fall within the range of 92% and 80%. Meta-substituted products, such as **4d**, **4l**, **4p**, and **4t**, exhibited a slight decrease in yields, situated between 89% and 73%. The ortho-substituted reactants behaved variably and spanned products **4h**, **4k**, **4q**, and **4u** from 77% down to 69%. Another distinct set, such as **4f**, **4p**, **4q**, **4v**, and **4w**, exhibited a very broad spectrum of yield, ranging from 91% to 57%.

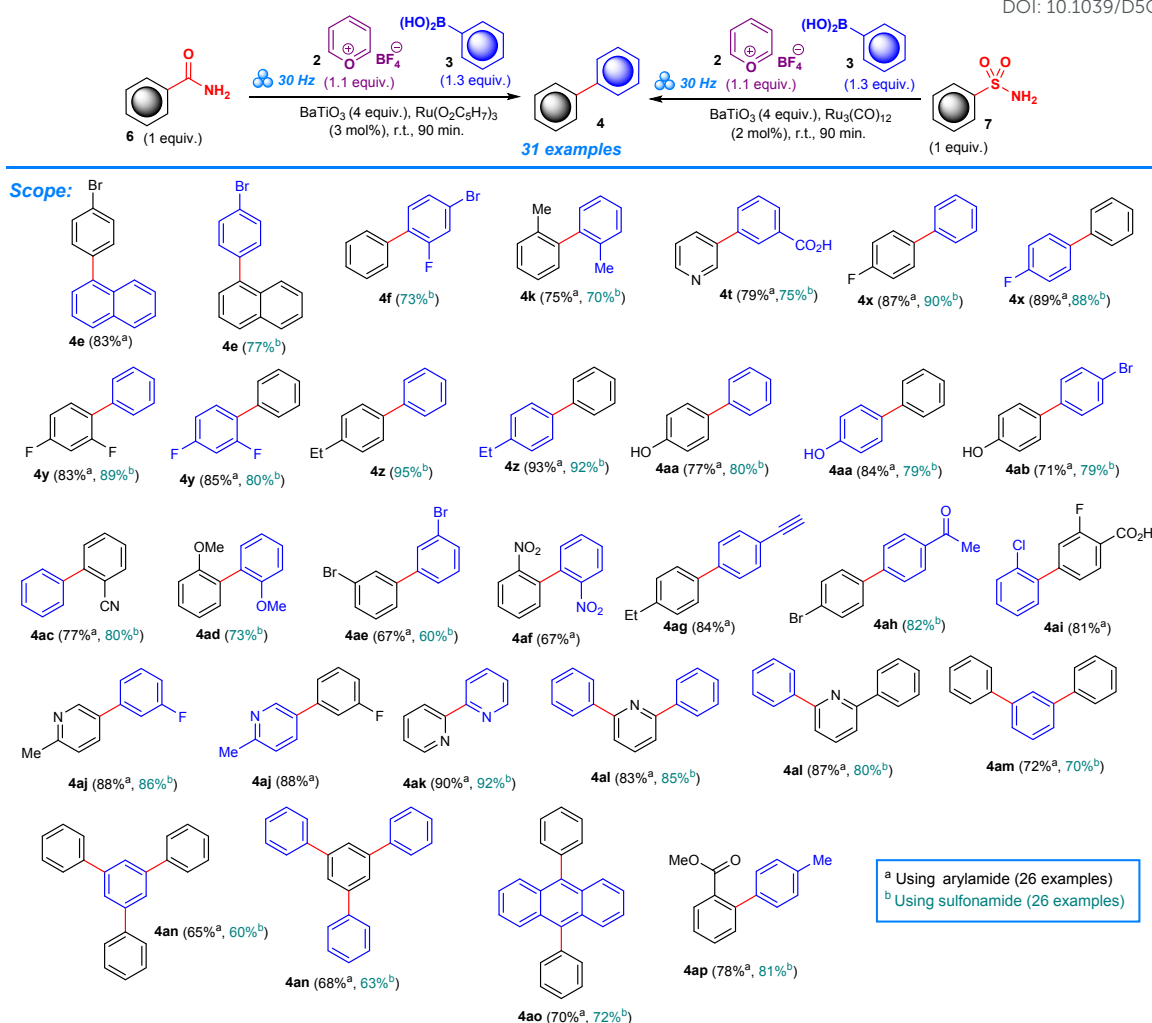
Similar trends were observed when trialkoxysilanes were used as coupling agents but with reduced efficiency (**Scheme 2**). The para-substituted reactants resulted in the highest yields, which ranged from 81% to 64% for: **4a–4c**, **4e**, **4g**, **4j**, **4m**, **4n**, **4r**. From the meta-positioned, only **4d** was attempted and this was at 78%. From ortho-substituted reactants, four compounds: **4f**, **4h**, **4k**, and **4q**, produced results ranging from 75% to 64%. Other substituent patterns, such as **4s**, **4e**, and **4t**, gave yields of 77%, 72%, and 60%, respectively, showing the strong effect of substituent placement on overall yield. Average yields for the different substituent groups over both series of reactions—involving either boronic acids or trialkoxysilanes—again reflect the observed trends. For the boronic acid series, average yields were about 85% for para, 82% for meta, 72% for ortho, and the separate group averaged about 73%. In the trialkoxysilane series, the average yields were lower, about 73% for para, 70% for ortho, the meta-substituted single example was 78%, and the other group averaged 70%. These averages show how much the substituent position influences yield results for the given reactions.

Inspired from the above successful outcomes, we embarked to examine the same synthetic scenario for the deaminative functionalization of amides and sulfonamides to produce biphenyls via extrusion of the carbonyl/sulfonyl moiety. With this intention, we replaced anilines from the above established model reactions, with aryl amide **6g** /sulfonamide **7h** as the model substrates and arylboronic acid **3a** as a coupling partner in presence of 3 equivalents of BaTiO<sub>3</sub> and 0.2 mL of 1,4-dioxane (**Table S3** and **S4**). Unfortunately, both the reactions failed to deliver the expected biaryls **4y/4z** (**Table S3** and **S4**, entry 1). The unexpected failure of the above experiments prompted us further to investigate the effect of transition metals in the proposed model reactions, as transition metals are one of the key components in most of the cross-coupling reactions. Thus, we began the investigation

performing both the model reactions with the additional presence of 5 mol% of an iron salt,  $\text{FeBr}_2(\text{CO})_4$ . Surprisingly, the biaryl product **4y** formed with 45% yield in case of the amide substrate **6g** (Table S3, entry 2) while the model reaction failed with sulfonamide **7h** as the starting material (Table S4, entry 2). It is well established that the ruthenium catalysts can catalyze decarbonylative cross-coupling reactions of variety of inert carbonyl functionalities (e.g. aldehydes, ketones, esters, and acid derivatives) via extrusion of the carbonyl moiety. Thus, purposely the efficacy of various Ru-complexes (5 mol%) has been tested as the catalysts in both the model reactions. The presence of  $\text{RuCl}_3 \cdot x\text{H}_2\text{O}$  in the reaction with amide substrate **6g** led the formation of the targeted biaryl product **4y** in 42% yield (Table S3, entry 3) while the same reaction did not proceed starting with sulfonamide **7h** (Table S4, entry 3). A significant decrease in the yields (from 39% to 11%) of biaryl **4y** was observed employing the respective Ru-complexes such as  $\text{RuCl}_2(\text{PPh}_3)_3$ ,  $[\text{Ru}(\text{NH}_3)_6]\text{Cl}_2$ ,  $(\text{PCy}_3)_2\text{Ru}(\text{=CHPh})(\text{Cl})_2$  [commonly known as first generation Grubbs catalyst] and  $\text{Ru}(\text{COD})\text{Cl}_2$  (Table S3, entries 4-7) while with the same Ru-complexes, the sulfonamide **7h** delivered the biaryl product **4z** in 18%, 0%, 34% and 0% yields respectively (Table S4, entries 4-7). Two more Ru-catalysts i.e.  $\text{Ru}_3(\text{CO})_{12}$  and  $\text{Ru}(\text{O}_2\text{C}_5\text{H}_7)_3$  have also been tested simultaneously in both the model reactions (Table S3 and S4, entries 8-9). Delightedly,  $\text{Ru}(\text{O}_2\text{C}_5\text{H}_7)_3$  found best in case of the model reaction with amide substrate **6g** delivering the expected biaryl compound **4y** in 85% yield (Table S3, entry 9), whereas  $\text{Ru}_3(\text{CO})_{12}$  gave excellent results with sulfonamide starting material **7h** yielding the respective biaryl product **4z** with 95% isolated yield (Table S4, entry 9). No change in the yields of the biaryls **4y** and **4z** were observed while performing the same model reactions in presence of the decreased amount, i.e. 3 mol% of the respective Ru-catalysts (Table S3 and S4, entry 10). A further decrease in the catalyst amount in the same model reactions led a drastic fall (up to less than half) in the yields of the respective biaryl products **4y** and **4z** (Table S3 and S4, entry 11). Thus, after a series of experiments the best optimization conditions are set as following: for the decarbonylative arylation of amide **6g**: Table S3, entry 10 and, for the desulfonamidative arylation of sulfonamide **7h**: Table S4, entry 10.

Likewise, the deaminative arylation of anilines, the above optimized reactions have also been screened in solution phase. The model reactions of aryl amide **6g** with arylboronic acid **3a** in various organic solvents under conventional heating/reflux conditions produce the biaryl product **4y** in the range of 0% to 33% yields (Table S3, entries 12-19) while the model reactions sulfonamide **7h** in the same organic media failed to deliver the expected biaryl **4z** (Table S4, entries 12-19). These results further highlight the importance of mechanochemical ball-milling over the conventional solution-based methods in the present methodologies.

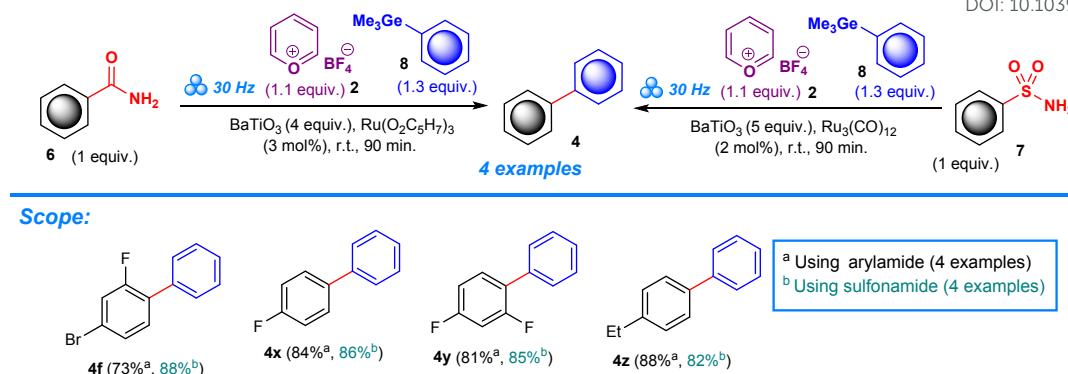
In Scheme 3, the scope was further extended to involve boronic acid as a coupling agent, trends characterized by moderate to high yields of product for aryl amides: 95% to 65% (**4e**, **4k**, **4x-4z**, **4aa-4ac**, **4ae-4ag**, **4ai-4ap**). Similar trends were observed for sulfonamides, albeit with reduced efficiency: 89% to 60% (**4e**, **4f**, **4k**, **4t**, **4x-4z**, **4aa-4ae**, **4ah**, **4aj**, **4ak-4ap**). Among the developed scope, seven such biaryls (**4e**, **4x-4z**, **4aa**, **4aj** and **4an**) have been synthesized by switching the aryl rings with amide/sulfonamide and arylboronic acid group or vice versa. Furthermore, the present strategy has been tested for the synthesis of two di- and tri-arylated cross-coupling products (**4al-4ao**) and 2,2'-bipyridine **4ak** with acceptable yields.



**Scheme 3.** Substrate scope for Ru-catalyzed cross-coupling of arylamides and sulfonamides with boronic acid for the synthesis of biphenyl derivatives.

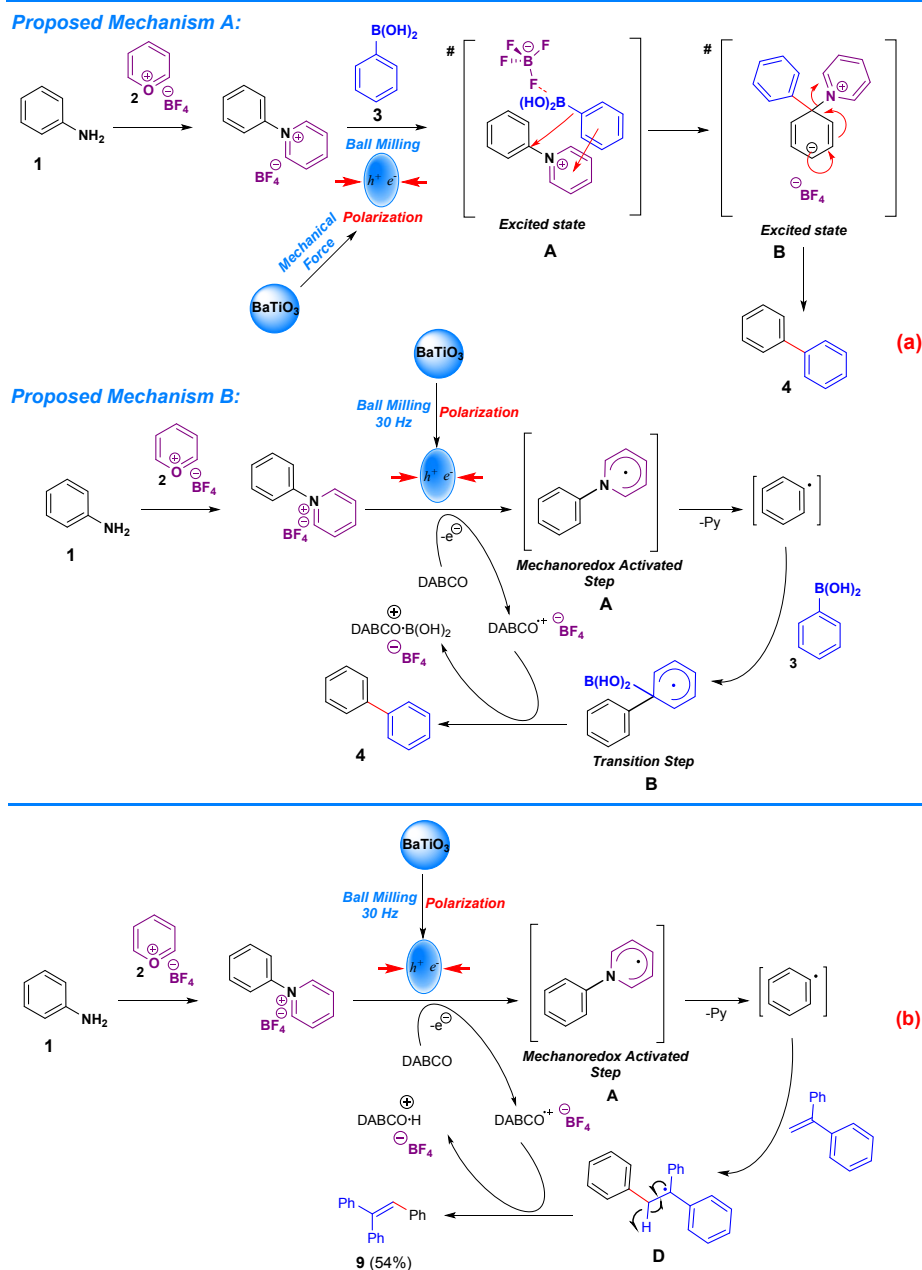
Inclusion of the ruthenium catalysts  $\text{Ru}(\text{O}_2\text{C}_5\text{H}_7)_3$  and  $\text{Ru}_3(\text{CO})_{12}$  expanded our scope to include the respective arylamides and sulfonamides functional groups, which undergo decarbonylative/desulfonamidative functionalization to the target biphenyls **4** (Scheme 4) using other coupling partner, aryl germane. Ratios of amides **1** or sulfonamides **2**, pyrylium tetrafluoroborate **2**, trimethyl(phenyl)germane **8**, and barium titanate  $\text{BaTiO}_3$  were included respectively as: 1 equivalent, 1.1 equivalents, 1.3 equivalents, and 4 equivalents; the optimized ruthenium catalyst i.e.  $\text{Ru}(\text{O}_2\text{C}_5\text{H}_7)_3$  or  $\text{Ru}_3(\text{CO})_{12}$  was added in 3 mol%. The presence of ruthenium catalyst ensures extrusion of the carbonyl moiety, CO, from amides and  $\text{SO}_2$  from sulfonamide functional groups.<sup>63</sup> A selection of products, **4f**, **4x**, **4y**, and **4z**, formed in moderate to high yield under the given conditions. For the reaction that employed arylamide as the starting reactant, the yields calculated to be 73%, 84%, 81%, and 88%, for each respective biphenyl derivative. The set of reactions which used sulfonamides reactant followed a similar trend in which product formation demonstrated high yields: 88%, 86%, 85%, and 82%. These results thus illustrate the capability of ruthenium catalysts to drive carbonyl or sulfonyl extrusion from the substrate, which in turn leads to a viable route to the selective functionalization of amides and sulfonamides in a one-pot mechanochemical setting.



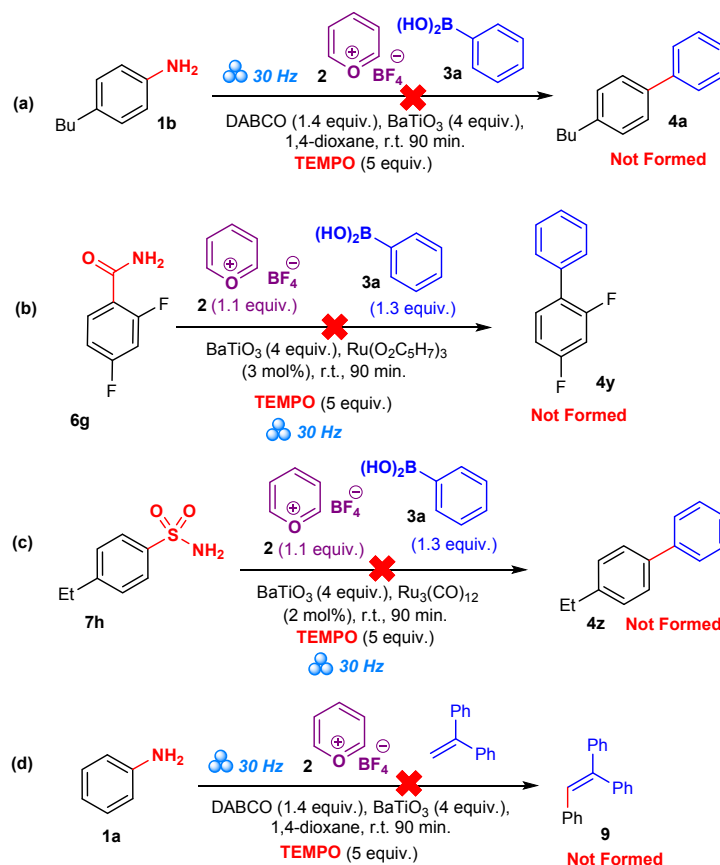


**Scheme 4.** Ru-catalyzed cross-coupling of arylamides and sulfonamides with trimethyl(phenyl)germanes.

Biphenyls are prepared by mechanochemically driven, transition-metal-free C–C coupling of boronic acids (or trialkoxysilanes) with aryl amines. Based on the above experimental outcomes, two plausible mechanistic pathways have been proposed, namely cationic and a radical mechanism (**Scheme 5**). As shown in **Scheme 5a** (part **A**), initially, the aniline derivative undergoes condensation with pyrylium tetrafluoroborate under the influence of mechanochemical ball-milling to generate the active pyridinium species.<sup>32, 47, 48</sup> The ball milling treatment causes mechanical stress and polarizes the barium titanate.<sup>53, 54, 64</sup> This mechanochemical polarization of barium titanate provides necessary energy input to excite the pyridinium intermediate to lead an excited state **A**, where the pyridinium intermediate undergoes a nucleophilic attack by boronic acid, resulting the formation of another excited state **B**. During the transformation from excited state **A** to **B**, the aryl group from the boronic acid forms a covalent bond with the *ipso* carbon of the N-aryl pyridinium intermediate. In the last step, the subsequent elimination of the pyridine moiety yields the of a biphenyl product. Structure **B** is the key because it allows direct arylation, which is usually challenging to effect without a transition metal catalyst. The other probable pathway of the mechanism could involve a mechanoredox process (**Scheme 5a** – part **B**). In the first step, aniline undergo condensation with pyrylium tetrafluoroborate, resulting in pyridinium species. The mechanochemical polarization of the piezoelectric material BaTiO<sub>3</sub> induces single-electron transfer (SET) from DABCO to the arylpyridinium intermediate generating the arylpyridine radical intermediate **A**, which acts as a synthetic equivalent for the formation of an aryl radical via elimination of pyridine molecule. This mechanoredox activation step opens a channel for arylation in the absence of a transition metal and hence realization of an alternative reaction pathway. The resulting arylpyridinium radical intermediate **A** adds to the *ipso* position of the arylboronic acid **3** leading to the formation of aryl radical transition state **B**. This step allows the direct coupling of an aryl group with the aromatic carbon without using a transition metal catalyst. Finally, the electron transfer from the transition state **B** to DABCO results o the formation of the expected biaryl product **4**, with DABCO cycling between its reduced and oxidized forms. In both mechanisms, this process is energy-driven, since the released energy is brought by barium titanate polarization. To confirm the mediation of the pyridinium salts, the reaction in **Scheme 5b** was conducted. A two-step, one-pot reaction of aniline and pyrylium tetrafluoroborate under standard conditions first gave the pyridinium salt and then, in the presence of ethene-1,1-diylidibenzene, gave the products of ethene-1,1,2-trinitrobenzene **6**; thus, we were able to intercept the formal phenyl cation and demonstrate the electrophilic character of the N-aryl pyridinium salts (**Scheme 5b** – steps: **C**, **D**). Noticeably, this method does not require transition metal catalysts, illuminating a more sustainable path to biphenyl compound synthesis from aryl amines.



**Scheme 5.** Proposed mechanisms of deaminative arylation of aryl amines. Proposal **A** is representative of a traditional nucleophilic route, whereas proposal **B** follows an alternative radical redox arylation cycle.



**Scheme 6.** Control experiments to validate the mechanism.

To validate the nature of proposed mechanism, four test reactions have been carried out starting with anilines, amide and sulfonamide with the respective coupling partner **3a** or **9** under the optimized reaction conditions, but with an additional presence of 5 equivalents of 2,2,6,6-tetramethylpiperidine 1-oxyl (TEMPO) (**Scheme 6**). Nevertheless, all these reactions failed to deliver the respective products confirming the involvement of the radical mechanism in the present transformations.

DFT calculations have been carried out to get insights into the proposed reaction mechanisms of deaminative arylation of aryl amines (**Scheme 5a**, mechanism path A and B), and the resulting energy profiles are presented in **Figure 1** and **Figure 2**. The **mechanism A** presents a traditional nucleophilic route and starts with the formation of a pyridinium intermediate involving reactants, i.e., aniline and pyridinium tetrafluoroborate. The obtained **Int1** lies at -10.72 kcal/mol with respect to initial reactants **R**. The pyridinium intermediate **Int1** undergoes arylation and thus **Int2** is formed through a nucleophilic attack by boronic acid. The **Int2** is -21.75 kcal/mol more stable with reference to **R**. The interaction distance between phenyl boronic acid and pyridinium intermediate at **int2** is 2.85 Å (C—C) while C—N bond distance elongated to 1.91 Å (**Int2**) from 1.45 Å (bare pyridinium intermediate). This nucleophilic attack undergoes through a transition state **TS1**. The activation barrier for this step is 23.30 kcal/mol. At the transition state i.e., **TS1**, the bond length of C—C bond decreases to 2.39 Å from 2.85 Å, while the C—N bond length increases to 2.30 Å from 1.91 Å (see **Figure 1**). The product of this step is **Int3**, where C—C bond length further decreases to 1.85 Å whereas the C—N bond length increases to 3.05 Å. The aryl group from the boronic acid forms a covalent bond with the *ipso* carbon of the N-aryl pyridinium intermediate. **Int3** is thermodynamically -63.75 kcal/mol more stable with respect to initial reactants. The conversion of **Int3** to **Int4** results in the removal of pyridine. **Int4** is located at -46.72 kcal/mol with respect to reactant **R**.

However, after **TS1** the boronic acid moiety B(OH)<sub>2</sub> remained with the reaction complex. Therefore, to detach boronic acid moiety with tetrafluoroborate, **Int3** undergoes a second transition state **TS2**. The **TS2** is located at the barrier height of 32.21 kcal/mol, which is easily accessible under mechanochemical conditions. The bond distance between boronic acid moiety and biphenyl (Ar—Ar) increases to 1.99 Å at **TS2** from 1.74 Å (**Int4**). Similarly, the product of **TS2** is obtained at -82.28 kcal/mol with respect to reference point **R** as **Int5**. After the **TS2**, in **Int5**, the bond distance between boronic acid and biphenyl (Ar—Ar) further increases, and bond distance of boronic acid to tetrafluoroborate further decreases resulting in the formation of biphenyl (**P**). The elimination of tetrafluoroborate boronic acid functionality yields the final biphenyl product. Therefore, establishing a fully mechanochemical pathway for the deaminative coupling of anilines, enabling the production of precursor biphenyl compounds.

Another mechanism i.e., **Mechanism B** follows an alternative radical redox arylation cycle for the formation of biphenyl. The initial step (till **Int1**) in **Mechanism B** are quite similar to **Mechanism A**, i.e., the formation of pyridinium intermediate. The polarization of

barium titanate results in monoradical electron transfer from DABCO to the pyridinium intermediate to form radical intermediate **Int2** which at -22.22 kcal/mol with respect to the reactants **R**. The subsequent step is the removal of pyridine moiety and formation of phenyl radical intermediate while going from **Int2** to **Int3**. **Int3** is thermodynamically -37.64 kcal/mol more stable with respect to **R**. The deamination of the aryl amine follows a radical pathway which upon direct coupling with the boronic acid, undergoes a transition step. Thus, **TS1** is located at the barrier height of 23.91 kcal/mol with respect to **Int4**. **Int4** is a stable specie involving boronic acid and a radical intermediate. At **TS1** the C—C bond distance between phenyl radical and phenyl boronic acid decreases to 2.11 Å from 2.31 Å. similarly the bond distance of B—C bond of aryl boronic acid increases from 1.65 Å to 1.73 Å (**Int4**) at the **TS1**. The product of this reaction is **Int5**, which is located at -63.23 kcal/mol with respect to **R**. Hence the radical mechanism allows the direct coupling of the aryl-aryl groups without using a transition metal catalyst. The B(OH)<sub>2</sub> leaves the **Int5**, resulting in the formation of final product **P**, i.e., biphenyl (Ar-Ar). The final biphenyl (Ar-Ar) product obtained in the mechanism is thermodynamically very stable i.e., lying at energy of -72.62 kcal/mol.

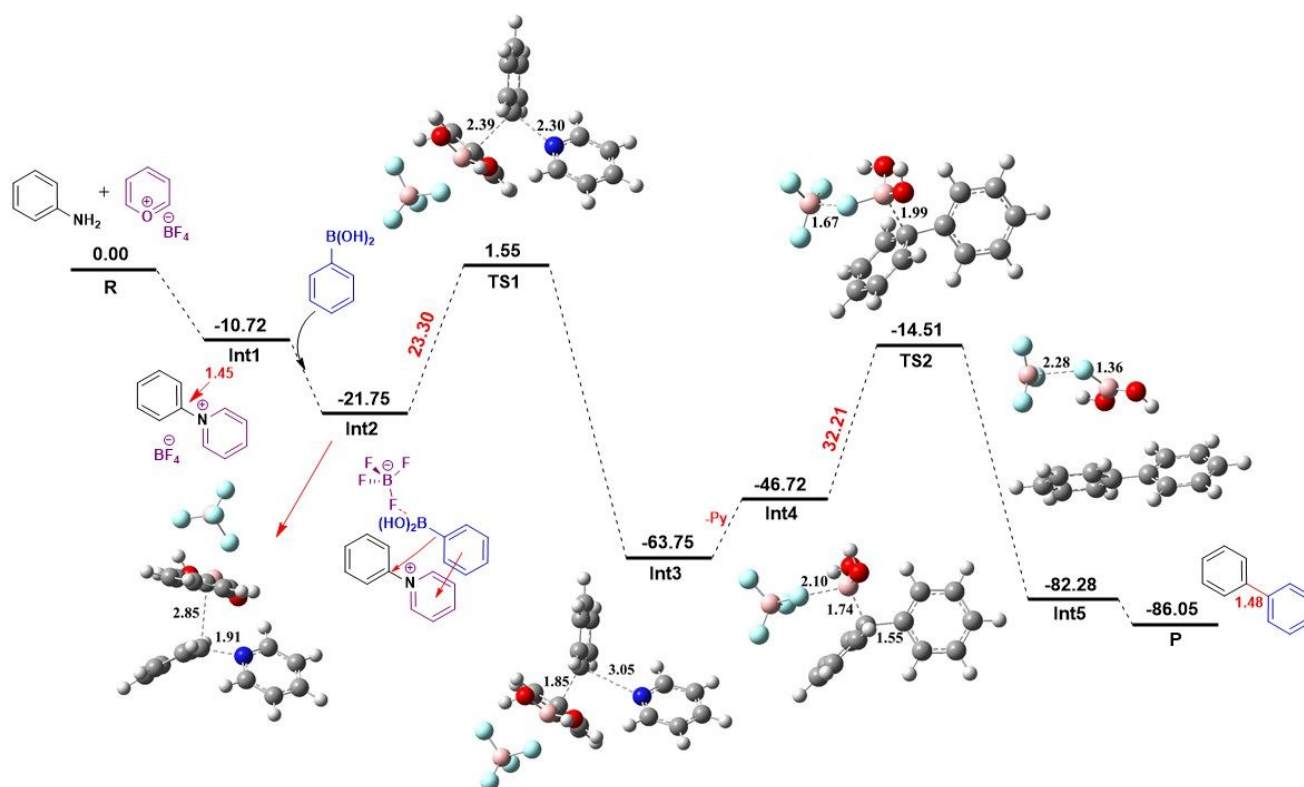


Figure 1. Free energy diagram of deaminative arylation of aryl amines through traditional nucleophilic route (Mechanism A, Scheme 5a). All the reported energy values are presented in kcal/mol with reference initial reactant (R) at 0.00 kcal/mol. Measured bond lengths are presented in Angstrom (Å).

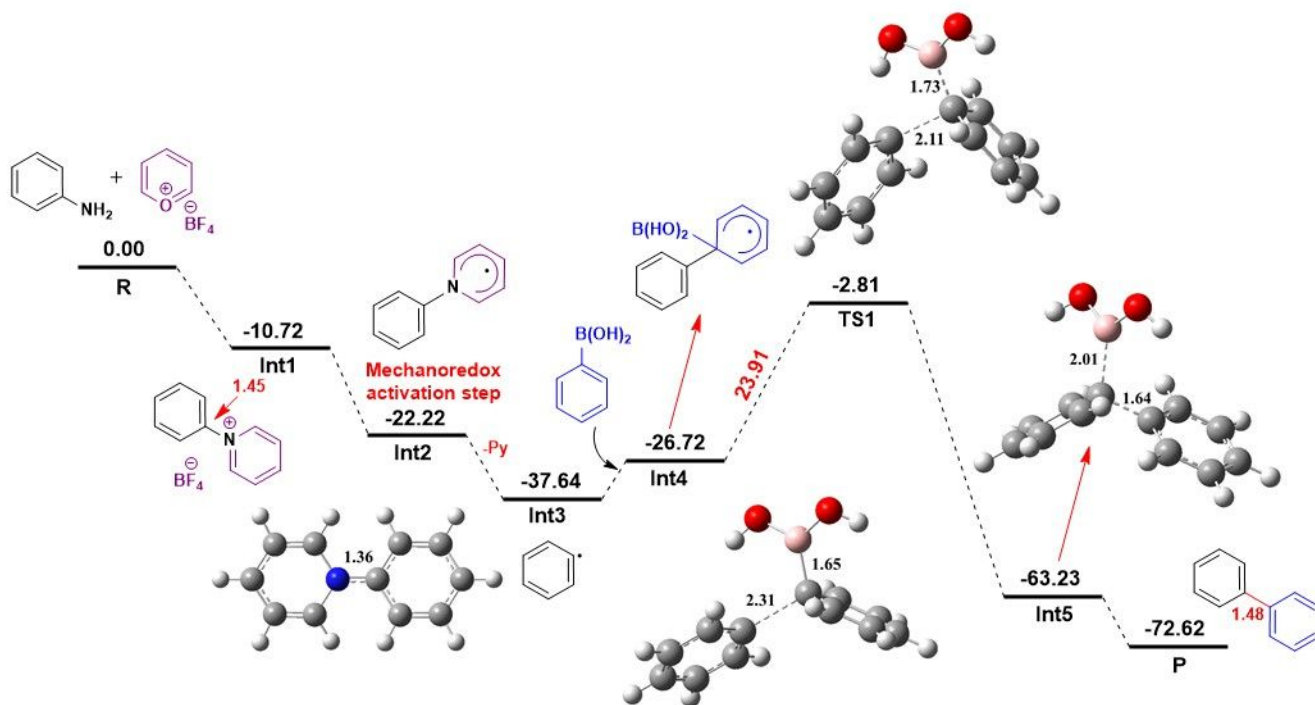
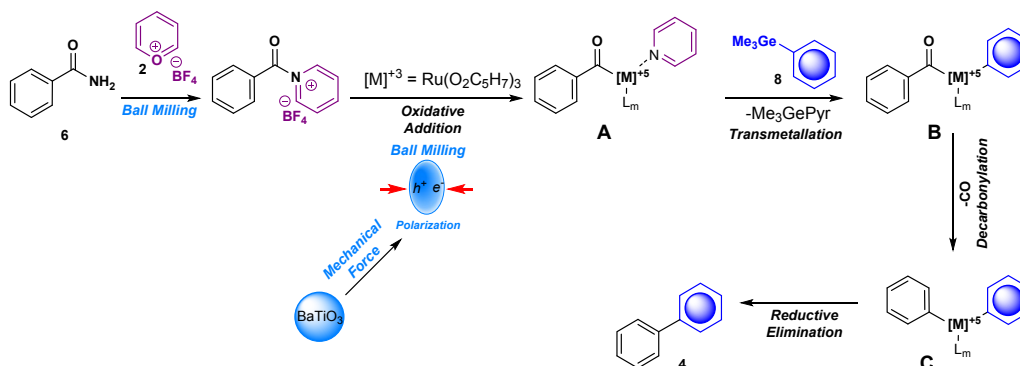


Figure 2. Free energy diagram of deaminative arylation of aryl amines through an alternative radical redox arylation cycle (Mechanism B, Scheme 5a). All the reported energy values are presented in kcal/mol with reference initial reactant (R) at 0.00 kcal/mol. Measured bond lengths are presented in Angstrom (Å).

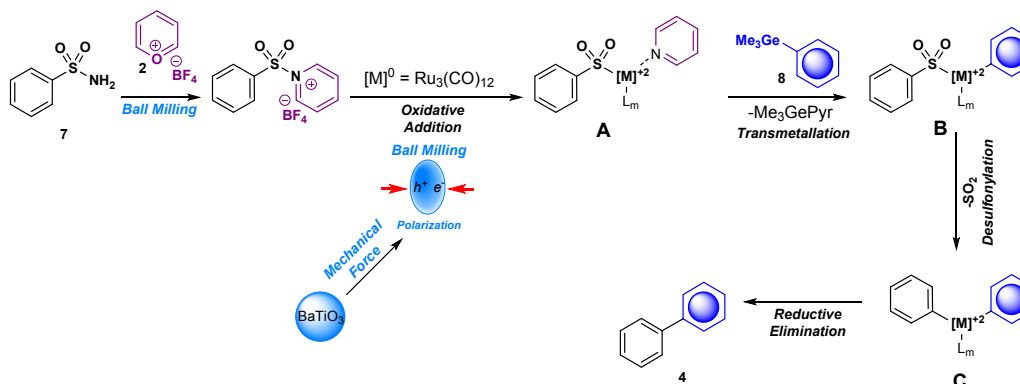
Based on the recent work by Chen et al.<sup>65</sup> and our studies on decarbonylative functionalization of aryl amides/sulfonamides,<sup>66, 67</sup> a separate mechanistic proposal was developed for the conversion of arylamides and sulfonamides into biphenyls as the presence of the ruthenium catalyst leads decarbonylative cross-coupling to biphenyl formation (**Scheme 7**). Aryl amide condensation ensues in presence of pyrylium tetrafluoroborate **2** to yield the acyl pyridinium intermediate, which is facilitated by mechanochemical ball milling. (**Scheme 7A**). The polarization of BaTiO<sub>3</sub> results in the activation of acyl pyridinium species which undergoes an oxidative insertion into the N-C(O) amide via insertion of ruthenium acetylacetonate [M]<sup>+3</sup> = Ru(O<sub>2</sub>C<sub>5</sub>H<sub>7</sub>)<sub>3</sub> to generate an acyl intermediate species **A**. The subsequent acylmetal intermediate undergoes direct transmetalation with a coupling agent (for example trimethyl(phenyl)germane **8**) via ligand exchange (intermediate **B**), followed by reductive elimination to furnish the acyl cross-coupling product. The acyl intermediate, which results from the selective oxidative addition of a low-valent metal into the N-C(O) amide bond leads to the extrusion of the carbonyl moiety (CO) and forms the intermediate complex **C**.<sup>63</sup> Finally, the process is completed by a reductive elimination to give cross-coupled biphenyl **4**. This process can be extended to include sulfonamides, which follow the same mechanistic pathway (**Scheme 7B**).



## A. Proposed Mechanism for Aryl Amide Conversion



## B. Proposed Mechanism for Sulfonamide Conversion



**Scheme 7.** Mechanistic proposal for decarbonylative/desulfonamidative arylation of aryl amides and sulfonamides.

The outcomes of the DFT calculations are much appropriate for the reactions which carried out in gaseous phase or in solution. It has been well established that mechanochemically induced reactions proceed along the synthetic pathways different from those described in the solution.<sup>68-71</sup> In solvothermal process the interaction between reactant molecules take place by collisions in liquid phase while in mechanochemical ball-milling process the reactants are grinded between the balls and vessel surface as well as the between the surface of balls, where the collision between the balls and the vessel supply the mechanical energy.<sup>68</sup>

During the mechanochemical ball milling, the substrates are subjected to the mechanical forces, such as shear and non-hydrostatic compression forces, and combinations thereof.<sup>72</sup> As a result, the solid reactants undergo several associated physical processes including particle size reduction (comminution), with a consequent surface area increase, and the formation of lattice defects of various types, wherein the reactivity is enhanced due to the reduction of the strength of the attractive interactions that hold the solid together, which also ultimately leads to amorphization. Furthermore, the mechanical energy acts synergistically with the internal energy of the chemical system due to its temperature, further increasing the chemical reactivity of the matter. Herein, the combined effects of grinding, crushing, pulverizing, impacting, and shearing forces can induce the chemical reactivity different from solution based processes.<sup>73</sup> These force-induced perturbations induce change in the energy landscape of chemical reactions and accelerate the dissociation of unloaded bonds and the changesets in the electronic configuration of covalent bonds, enabling a different chemical selectivity than conventional solution-based reactions. Moreover, the ball-milling process ensures the feasibility of the reaction by the creation of hot spots (which has temperature about 600-1000 K), enhanced solid-solid mixing and contact area, the creation of meta-stable or unstable structural configurations, or producing reactive surfaces in situ.<sup>68</sup> Thus, by managing the milling parameters, such as the ball/powder weight ratio, milling frequency, milling time, and atmosphere, it is possible to drive the kinetics of mechanochemical reactions to overcome the energy barrier which is quite difficult in solution phase processes.

## Conclusion

In the present study, mechanochemical deaminative arylation of C–N in anilines, aryl amides, and sulfonamides has been introduced as a new gateway towards novel synthesis of biphenyls. This conversion results in formation of reactive pyridinium salts intermediates by pyrylium tetrafluoroborate condensation followed by direct coupling. This represents a greener methodology for synthesis compared to traditional transition-metal-catalysis-based methods. Successful incorporation of arylamides and

sulfonamides results *via* incorporation of a ruthenium catalysts, enabling decarbonylative/desulfonylative cross-coupling for selective arylation to achieve moderate to high yields of biphenyls. Substituent position on the reactant and coupling agent influences the yields of the reaction, with para-substituted reactants having the highest average yield in couplings performed with boronic acids. The meta and ortho-substituted amines gave slightly lower yields. Couplings to trialkoxysilane followed a similar trend but with generally lower yields.

### Contribution statement

Conceptualization: S. M., V. O. I.; methodology: S. M., V. O. I.; investigation: S. M., M. G. G., S. S., K. A., S. K., G. A., J. F., M.S., V. B. P., J. Z., E. K., B. B., V. O. I.; writing – original draft: M. G. G., V. B. P., S. M., and V. O. I.; writing – review & editing: M. G. G., V. B. P., S. M., and V. O. I.; funding acquisition: S. M., V. O. I.; resources: S. M., V. O. I.; supervision: S. M., V. O. I.

### Supporting Information

The Supporting Information is available free of charge at:

General information, synthetic procedures, spectral data, and copies of  $^1\text{H}$  and  $^{13}\text{C}\{^1\text{H}\}$  NMR (PDF)

### Acknowledgements

This work was supported by the Slovak Research and Development Agency under the Contract no. APVV-21-0362.

### REFERENCES

1. Eastgate, M. D.; Schmidt, M. A.; Fandrick, K. R., Erratum: On the design of complex drug candidate syntheses in the pharmaceutical industry. *Nature Reviews Chemistry* **2017**, *1* (2), 0016.
2. Varenikov, A.; Shapiro, E.; Gandelman, M., Decarboxylative Halogenation of Organic Compounds. *Chemical Reviews* **2021**, *121* (1), 412-484.
3. Chen, H.; Liu, Y. A.; Liao, X., Recent Progress in Radical Decarboxylative Functionalizations Enabled by Transition-Metal (Ni, Cu, Fe, Co or Cr) Catalysis. *Synthesis* **2020**, *53* (01), 1-29.
4. Sun, C.-L.; Shi, Z.-J., Transition-Metal-Free Coupling Reactions. *Chemical Reviews* **2014**, *114* (18), 9219-9280.
5. Qiu, Z.; Li, C.-J., Transformations of Less-Activated Phenols and Phenol Derivatives via C–O Cleavage. *Chemical Reviews* **2020**, *120* (18), 10454-10515.
6. Nakao, Y., Metal-mediated C–CN Bond Activation in Organic Synthesis. *Chemical Reviews* **2021**, *121* (1), 327-344.
7. Korch, K. M.; Watson, D. A., Cross-Coupling of Heteroatomic Electrophiles. *Chemical Reviews* **2019**, *119* (13), 8192-8228.
8. Cherney, A. H.; Kadunce, N. T.; Reisman, S. E., Enantioselective and Enantiospecific Transition-Metal-Catalyzed Cross-Coupling Reactions of Organometallic Reagents To Construct C–C Bonds. *Chemical Reviews* **2015**, *115* (17), 9587-9652.
9. Brenk, R.; Schipani, A.; James, D.; Krasowski, A.; Gilbert, I. H.; Frearson, J.; Wyatt, P. G., Lessons Learnt from Assembling Screening Libraries for Drug Discovery for Neglected Diseases. *ChemMedChem* **2008**, *3* (3), 435-444.
10. Schneider, G., Automating drug discovery. *Nature Reviews Drug Discovery* **2018**, *17* (2), 97-113.
11. Campos, K. R.; Coleman, P. J.; Alvarez, J. C.; Dreher, S. D.; Garbaccio, R. M.; Terrett, N. K.; Tillyer, R. D.; Truppo, M. D.; Parmee, E. R., The importance of synthetic chemistry in the pharmaceutical industry. *Science* **2019**, *363* (6424), eaat0805.
12. Mkrtchyan, S.; Shkoo, M.; Phanindrudu, M.; Medved', M.; Sevastyanova, O.; Iaroshenko, V. O., Mechanochemical Defluorinative Arylation of Trifluoroacetamides: An Entry to Aromatic Amides. *The Journal of Organic Chemistry* **2023**, *88* (2), 863-870.
13. Mkrtchyan, S.; Jakubczyk, M.; Lanka, S.; Pittelkow, M.; Iaroshenko, V. O., Cu-Catalyzed Arylation of Bromo-Difluoro-Acetamides by Aryl Boronic Acids, Aryl Trialkoxysilanes and Dimethyl-Aryl-Sulfonium Salts: New Entries to Aromatic Amides. *Molecules* **2021**, *26* (10), 2957.
14. Boit, T. B.; Bulger, A. S.; Dander, J. E.; Garg, N. K., Activation of C–O and C–N Bonds Using Non-Precious-Metal Catalysis. *ACS Catalysis* **2020**, *10* (20), 12109-12126.
15. Ahrens, T.; Kohlmann, J.; Ahrens, M.; Braun, T., Functionalization of Fluorinated Molecules by Transition-Metal-Mediated C–F Bond Activation To Access Fluorinated Building Blocks. *Chemical Reviews* **2015**, *115* (2), 931-972.
16. Knapp, R. R.; Bulger, A. S.; Garg, N. K., Nickel-Catalyzed Conversion of Amides to Carboxylic Acids. *Organic Letters* **2020**, *22* (7), 2833-2837.
17. Zou, X.; Shen, B.; Li, G.-L.; Liang, Q.; Ouyang, Y.; Yang, B.; Yu, P.; Gao, B., Strain-promoted S-arylation and alkenylation of sulfinamides using arynes and cyclic alkynes. *Science China Chemistry* **2024**, *67* (3), 928-935.
18. Ricci, A., Amino Group Chemistry: From Synthesis to the Life Sciences. **2007**.

19. Luo, Y.-R., Comprehensive Handbook of Chemical Bond Energies. **2007**, 1688.
20. Berger, K. J.; Levin, M. D., Reframing primary alkyl amines as aliphatic building blocks. *Organic & Biomolecular Chemistry* **2021**, *19* (1), 11-36.
21. Broeckaert, L.; Moens, J.; Roos, G.; Proft, F. D.; Geerlings, P., Intrinsic Nucleofugality Scale within the Framework of Density Functional Reactivity Theory. *The Journal of Physical Chemistry A* **2008**, *112* (47), 12164-12171.
22. Kong, D.; Moon, P. J.; Lundgren, R. J., Radical coupling from alkyl amines. *Nature Catalysis* **2019**, *2* (6), 473-476.
23. Laurence, C.; Brameld, K. A.; Graton, J.; Le Questel, J.-Y.; Renault, E., The pKBHX Database: Toward a Better Understanding of Hydrogen-Bond Basicity for Medicinal Chemists. *Journal of Medicinal Chemistry* **2009**, *52* (14), 4073-4086.
24. Wu, G.; Deng, Y.; Wu, C.; Zhang, Y.; Wang, J., Synthesis of  $\alpha$ -Aryl Esters and Nitriles: Deaminative Coupling of  $\alpha$ -Aminoesters and  $\alpha$ -Aminoacetonitriles with Arylboronic Acids. *Angewandte Chemie International Edition* **2014**, *53* (39), 10510-10514.
25. He, L.; Qiu, G.; Gao, Y.; Wu, J., Removal of amino groups from anilines through diazonium salt-based reactions. *Organic & Biomolecular Chemistry* **2014**, *12* (36), 6965-6971.
26. Wang, D.-Y.; Yang, Z.-K.; Wang, C.; Zhang, A.; Uchiyama, M., From Anilines to Aryl Ethers: A Facile, Efficient, and Versatile Synthetic Method Employing Mild Conditions. *Angewandte Chemie International Edition* **2018**, *57* (14), 3641-3645.
27. Reeves, J. T.; Fandrick, D. R.; Tan, Z.; Song, J. J.; Lee, H.; Yee, N. K.; Senanayake, C. H., Room Temperature Palladium-Catalyzed Cross Coupling of Aryltrimethylammonium Triflates with Aryl Grignard Reagents. *Organic Letters* **2010**, *12* (19), 4388-4391.
28. Rand, Alexander W.; Montgomery, J., Catalytic reduction of aryl trialkylammonium salts to aryl silanes and arenes. *Chemical Science* **2019**, *10* (20), 5338-5344.
29. Wang, D.-Y.; Kawahata, M.; Yang, Z.-K.; Miyamoto, K.; Komagawa, S.; Yamaguchi, K.; Wang, C.; Uchiyama, M., Stille coupling via C-N bond cleavage. *Nature Communications* **2016**, *7* (1), 12937.
30. He, R.-D.; Li, C.-L.; Pan, Q.-Q.; Guo, P.; Liu, X.-Y.; Shu, X.-Z., Reductive Coupling between C-N and C-O Electrophiles. *Journal of the American Chemical Society* **2019**, *141* (32), 12481-12486.
31. Katritzky, A. R., Conversions of primary amino groups into other functionality mediated by pyrylium cations. *Tetrahedron* **1980**, *36* (6), 679-699.
32. Katritzky, A. R.; Marson, C. M., Pyrylium Mediated Transformations of Primary Amino Groups into Other Functional Groups. New Synthetic Methods (41). *Angewandte Chemie International Edition in English* **1984**, *23* (6), 420-429.
33. Yousif, A. M.; Colarusso, S.; Bianchi, E., Katritzky Salts for the Synthesis of Unnatural Amino Acids and Late-Stage Functionalization of Peptides. *European Journal of Organic Chemistry* **2023**, *26* (12), e202201274.
34. Pang, Y.; Moser, D.; Cornella, J., Pyrylium Salts: Selective Reagents for the Activation of Primary Amino Groups in Organic Synthesis. *Synthesis* **2020**, *52* (04), 489-503.
35. M. Correia, J. T.; A. Fernandes, V.; Matsuo, B. T.; C. Delgado, J. A.; de Souza, W. C.; Paixão, M. W., Photoinduced deaminative strategies: Katritzky salts as alkyl radical precursors. *Chemical Communications* **2020**, *56* (4), 503-514.
36. Huang, J.; Zhang, L.; Meng, X., Recent advances in the cyclization reactions of pyridinium 1,n-zwitterions (n = 4 and 5): scope and mechanism. *Organic Chemistry Frontiers* **2023**, *10* (11), 2813-2829.
37. Roychowdhury, P.; Samanta, S.; Tan, H.; Powers, D. C., N-Amino pyridinium salts in organic synthesis. *Organic Chemistry Frontiers* **2023**, *10* (10), 2563-2580.
38. Li, Y.-N.; Xiao, F.; Guo, Y.; Zeng, Y.-F., Recent Developments in Deaminative Functionalization of Alkyl Amines. *European Journal of Organic Chemistry* **2021**, *2021* (8), 1215-1228.
39. Sowmiah, S.; Esperança, J. M. S. S.; Rebelo, L. P. N.; Afonso, C. A. M., Pyridinium salts: from synthesis to reactivity and applications. *Organic Chemistry Frontiers* **2018**, *5* (3), 453-493.
40. Hoerrner, M. E.; Baker, K. M.; Basch, C. H.; Bampo, E. M.; Watson, M. P., Deaminative Arylation of Amino Acid-derived Pyridinium Salts. *Organic Letters* **2019**, *21* (18), 7356-7360.
41. Basch, C. H.; Liao, J.; Xu, J.; Piane, J. J.; Watson, M. P., Harnessing Alkyl Amines as Electrophiles for Nickel-Catalyzed Cross Couplings via C-N Bond Activation. *Journal of the American Chemical Society* **2017**, *139* (15), 5313-5316.
42. Liao, J.; Guan, W.; Boscoe, B. P.; Tucker, J. W.; Tomlin, J. W.; Garnsey, M. R.; Watson, M. P., Transforming Benzylic Amines into Diarylmethanes: Cross-Couplings of Benzylic Pyridinium Salts via C-N Bond Activation. *Organic Letters* **2018**, *20* (10), 3030-3033.
43. Guan, W.; Liao, J.; Watson, M. P., Vinylation of Benzylic Amines via C-N Bond Functionalization of Benzylic Pyridinium Salts. *Synthesis* **2018**, *50* (16), 3231-3237.
44. Ghiazza, C.; Faber, T.; Gómez-Palomino, A.; Cornella, J., Deaminative chlorination of aminoheterocycles. *Nature Chemistry* **2022**, *14* (1), 78-84.
45. Ghiazza, C.; Faber, T.; Gómez-Palomino, A.; Cornella, J., Author Correction: Deaminative chlorination of aminoheterocycles. *Nature Chemistry* **2022**, *14* (5), 582-582.
46. Ghiazza, C.; Wagner, L.; Fernández, S.; Leutzsch, M.; Cornella, J., Bio-Inspired Deaminative Hydroxylation of Aminoheterocycles and Electron-Deficient Anilines. *Angewandte Chemie International Edition* **2023**, *62* (2), e202212219.

47. Moser, D.; Duan, Y.; Wang, F.; Ma, Y.; O'Neill, M. J.; Cornella, J., Selective Functionalization of Aminoheterocycles by a Pyrylium Salt. *Angewandte Chemie International Edition* **2018**, *57* (34), 11035-11039.
48. Jakubczyk, M.; Mkrtchyan, S.; Shkooor, M.; Lanka, S.; Budzák, Š.; Iliaš, M.; Skoršepa, M.; Iaroshenko, V. O., Mechanochemical Conversion of Aromatic Amines to Aryl Trifluoromethyl Ethers. *Journal of the American Chemical Society* **2022**, *144* (23), 10438-10445.
49. Mkrtchyan, S.; Purohit, V. B.; Shalimov, O.; Zapletal, J.; Sarfaraz, S.; Ayub, K.; Filo, J.; Sillanpää, M.; Skoršepa, M.; Iaroshenko, V. O., Mechanochemical Synthesis of Trifluoromethyl Arenes: Nanocellulose-Supported Deaminative Trifluoromethylation of Aromatic Amines. *ACS Sustainable Chemistry & Engineering* **2024**, *12* (24), 8980-8989.
50. Mkrtchyan, S.; Shalimov, O.; Purohit, V. B.; Zapletal, J.; Prajapati, V. D.; Prajapati, R. V.; Elumalai, D.; Garcia, M. G.; Filo, J.; Addová, G.; Benická, B.; Iaroshenko, V. O., Nanocellulose as Reaction Medium for FeCl<sub>3</sub>-Mediated Mechanochemical Deaminative Fluorination of (Hetero)aromatic Amines. *Advanced Synthesis & Catalysis* **2024**, *366* (15), 3269-3276.
51. Mkrtchyan, S.; Jakubczyk, M.; Lanka, S.; Yar, M.; Ayub, K.; Shkooor, M.; Pittelkow, M.; Iaroshenko, V. O., Mechanochemical Transformation of CF<sub>3</sub> Group: Synthesis of Amides and Schiff Bases. *Advanced Synthesis & Catalysis* **2021**, *363* (24), 5448-5460.
52. Mkrtchyan, S.; Purohit, V. B.; Khutsishvili, S.; Nociarová, J.; Yar, M.; Mahmood, T.; Ayub, K.; Budzák, Š.; Skoršepa, M.; Iaroshenko, V. O., Mechanochemical Defluorinative Acylation of ortho-Hydroxyarylenaminones by CF<sub>3</sub>-Compounds: Synthesis of 3-Acylchromones. *Advanced Synthesis & Catalysis* **2023**, *365* (12), 2026-2035.
53. Seo, T.; Kubota, K.; Ito, H., Dual Nickel(II)/Mechanoredox Catalysis: Mechanical-Force-Driven Aryl-Amination Reactions Using Ball Milling and Piezoelectric Materials. *Angewandte Chemie International Edition* **2023**, *62* (42), e202311531.
54. Kubota, K.; Pang, Y.; Miura, A.; Ito, H., Redox reactions of small organic molecules using ball milling and piezoelectric materials. *Science* **2019**, *366* (6472), 1500-1504.
55. Schumacher, C.; Hernández, J. G.; Bolm, C., Electro-Mechanochemical Atom Transfer Radical Cyclizations using Piezoelectric BaTiO<sub>3</sub>. *Angewandte Chemie International Edition* **2020**, *59* (38), 16357-16360.
56. Howard, Joseph L.; Cao, Q.; Browne, D. L., Mechanochemistry as an emerging tool for molecular synthesis: what can it offer? *Chemical Science* **2018**, *9* (12), 3080-3094.
57. Štrukil, V.; Igrc, M. D.; Fábíán, L.; Eckert-Maksić, M.; Childs, S. L.; Reid, D. G.; Duer, M. J.; Halasz, I.; Mottillo, C.; Frišić, T., A model for a solvent-free synthetic organic research laboratory: click-mechanosynthesis and structural characterization of thioureas without bulk solvents. *Green Chemistry* **2012**, *14* (9), 2462-2473.
58. Genchi, G.; Carocci, A.; Lauria, G.; Sinicropi, M. S.; Catalano, A. Nickel: Human Health and Environmental Toxicology *International Journal of Environmental Research and Public Health* [Online], 2020.
59. Balaram, V., Environmental Impact of Platinum, Palladium, and Rhodium Emissions from Autocatalytic Converters – A Brief Review of the Latest Developments. In *Handbook of Environmental Materials Management*, Hussain, C. M., Ed. Springer International Publishing: Cham, 2020; pp 1-37.
60. Halasz, I.; Kimber, S. A. J.; Beldon, P. J.; Belenguer, A. M.; Adams, F.; Honkimäki, V.; Nightingale, R. C.; Dinnebier, R. E.; Frišić, T., In situ and real-time monitoring of mechanochemical milling reactions using synchrotron X-ray diffraction. *Nature Protocols* **2013**, *8* (9), 1718-1729.
61. Mateti, S.; Mathesh, M.; Liu, Z.; Tao, T.; Ramireddy, T.; Glushenkov, A. M.; Yang, W.; Chen, Y. I., Mechanochemistry: A force in disguise and conditional effects towards chemical reactions. *Chemical Communications* **2021**, *57* (9), 1080-1092.
62. Flessner, T.; Doye, S., Cesium carbonate: A powerful inorganic base in organic synthesis. *Journal für praktische Chemie* **1999**, *341* (2), 186-190.
63. Liu, C.; Szostak, M., Decarbonylative cross-coupling of amides. *Organic & Biomolecular Chemistry* **2018**, *16* (43), 7998-8010.
64. Xia, H.; Wang, Z., Piezoelectricity drives organic synthesis. *Science* **2019**, *366* (6472), 1451-1452.
65. Chen, H.; Chen, D.-H.; Huang, P.-Q., Heteroaromatization and nickel catalysis enabled decarbamoylative arylations and borylations of tertiary amides. *Cell Reports Physical Science* **2023**, *4* (9), 101574.
66. Mkrtchyan, S.; Purohit, V. B.; Shalimov, O.; Jakubczyk, M.; Prajapati, V. D.; Prajapati, R. V.; Zapletal, J.; Karpun, Y.; Yepishev, V.; Addová, G.; Filo, J.; Kupcová, E.; Benická, B.; Kmeťová, J.; Iaroshenko, V. O., Mechanochemical decarbonylative transformation of the amide group into OCF<sub>3</sub> and CF<sub>3</sub> functionalities under ruthenium catalysis. *Organic Chemistry Frontiers* **2025**, *12* (4), 1189-1198.
67. Mkrtchyan, S.; Purohit, V. B.; Prajapati, V. D.; Prajapati, R. V.; Shalimov, O.; Sarfaraz, S.; Ayub, K.; Iaroshenko, V. O., Ruthenium Catalyzed Mechanochemical Transformation of Sulfonamide Group to Fluoro, Trifluoromethyl, and Trifluoromethoxy Functionalities. *Chemistry - An Asian Journal* **2025**, *20* (12), e202500221.
68. Tricker, A. W.; Samaras, G.; Hebisch, K. L.; Realf, M. J.; Sievers, C., Hot spot generation, reactivity, and decay in mechanochemical reactors. *Chem. Eng. J.* **2020**, *382*, 122954.
69. Templ, J.; Schnürch, M., High-Energy Ball Milling Enables an Ultra-Fast Wittig Olefination Under Ambient and Solvent-free Conditions. *Angew. Chem. Int. Ed.* **2024**, *63* (49), e202411536.
70. Takacs, L., The historical development of mechanochemistry. *Chem. Soc. Rev.* **2013**, *42* (18), 7649-7659.

71. Narayanan, N. K.; Schnürch, M., Mechanochemical Ball Milling Approach to C(sp<sup>3</sup>)-H Functionalization of 8-Methylquinolines. *ChemCatChem* **2025**, *17* (5), e202401613.

72. Pagola, S., Outstanding Advantages, Current Drawbacks, and Significant Recent Developments in Mechanochemistry: A Perspective View. *Crystals* **2023**, *13* (1), 124.

73. Cuccu, F.; De Luca, L.; Delogu, F.; Colacino, E.; Solin, N.; Mocci, R.; Porcheddu, A., Mechanochemistry: New Tools to Navigate the Uncharted Territory of “Impossible” Reactions. *ChemSusChem* **2022**, *15* (17), e202200362.



## Data Availability Statement

The datasets supporting this article have been uploaded as part of the ESI, it encompasses general information, synthetic procedures, spectral data, and copies of  $^1\text{H}$  and  $^{13}\text{C}\{^1\text{H}\}$  NMR (PDF).